

Aging solitons in photorefractive dipolar glasses

J. Parravicini,^{1,2} D. Pierangeli,¹ F. Di Mei,^{1,3} C. Conti,^{1,4} A. J. Agranat,⁵ and E. DelRe^{1,2,*}

¹ Department of Physics, University of Rome "La Sapienza", 00185 Rome, Italy

² IPCF-CNR, University of Rome "La Sapienza", 00185 Rome, Italy

³ Center for Life Nano Science@Sapienza, Istituto Italiano di Tecnologia, 00161 Rome, Italy

⁴ ISC-CNR, University of Rome "La Sapienza", 00185 Rome, Italy

⁵ Applied Physics Department, Hebrew University of Jerusalem, 91904 Israel

*eugenio.delre@uniroma1.it

Abstract: We study experimentally the aging of optical spatial solitons in a dipolar glass hosted by a nanodisordered sample of photorefractive potassium-sodium-tantalate-niobate (KNTN). As the system ages, the waves erratically explore varying strengths of the nonlinear response, causing them to break up and scatter. We show that this process can still lead to solitons, but in a generalized form for which the changing response is compensated by changing the normalized wave size and intensity so as to maintain fixed the optical waveform.

© 2013 Optical Society of America

OCIS codes: (160.2750) Glass and other amorphous materials; (190.4400) Nonlinear optics, materials; (190.5330) Photorefractive optics.

References and links

1. E. Donth, *The Glass Transition* (Springer, 2001).
2. L. Leuzzi and T. M. Nieuwenhuizen, *Thermodynamics of the Glassy State* (Taylor and Francis, 2008).
3. C. A. Angell, "Glass-formers and viscous liquid slowdown since David Turnbull: Enduring puzzles and new twists," *MRS Bull.* **33**, 544–555 (2008).
4. N. Gofraniha, C. Conti, and G. Ruocco, "Aging of the nonlinear optical susceptibility in doped colloidal suspensions," *Phys. Rev. B* **75**, 224203 (2007).
5. N. Gofraniha, C. Conti, G. Ruocco, and F. Zamponi, "Time-dependent nonlinear optical susceptibility of an out-of-equilibrium soft material," *Phys. Rev. Lett.* **102**, 038303 (2009).
6. G. A. Samara, "The relaxational properties of compositionally disordered ABO₃ perovskites," *J. Phys. Condens. Matter* **15**, R367–R411 (2003).
7. A. Bokov, "Recent progress in relaxor ferroelectrics with perovskite structure," *J. Mater. Sci.* **41**, 31–52 (2006).
8. P. Ben Ishai, C. E. M. De Olivera, Y. Ryabov, Y. Feldman, and A. J. Agranat, "Glass-forming liquid kinetics manifested in a KTN:Cu crystal," *Phys. Rev. B* **70**, 132104 (2004).
9. A. Gumennik, Y. Kurzweil-Segev, and A. J. Agranat, "Electrooptical effects in glass forming liquids of dipolar nano-clusters embedded in a paraelectric environment," *Opt. Mater. Express* **1**, 332–343 (2011).
10. Y. Chang, C. Wang, S. Yin, R. C. Hoffman, and A. G. Mott, "Kovacs effect enhanced broadband large field of view electro-optic modulators in nanodisordered KTN crystals," *Opt. Express* **21**, 17760–17768 (2013).
11. C. Hu, H. Tian, B. Yao, Z. Zhou, and D. Chen, "Large quadratic electro-optic effect in K_{0.99}Li_{0.01}Ta_{0.60}Nb_{0.40}O₃ single crystal," *Curr. Appl. Phys.* **13**, 785–788 (2013).
12. G. Bitton, Y. Feldman, and A. J. Agranat, "Relaxation processes of off-center impurities in KTN:Li crystals," *J. Non-Cryst. Solids* **305**, 362–367 (2002).
13. E. DelRe, E. Spinozzi, A. J. Agranat, and C. Conti, "Scale-free optics and diffractionless waves in nanodisordered ferroelectrics," *Nat. Photonics* **5**, 39–42 (2011).
14. E. DelRe and C. Conti, "Scale-free optics," in *Nonlinear Photonics and Novel Optical Phenomena*, Vol. 170 of Springer Series in Optical Sciences (Springer, 2012), Chap. 8, pp. 207–230.

15. J. Parravicini, F. Di Mei, C. Conti, A.J. Agranat, and E. DelRe, "Diffraction cancellation over multiple wavelengths in photorefractive dipolar glasses," *Opt. Express* **19**, 24109–24114 (2011).
16. J. Parravicini, C. Conti, A. J. Agranat, and E. DelRe, "Rejuvenation in scale-free optics and enhanced diffraction cancellation life-time," *Opt. Express* **20**, 27382–27387 (2012).
17. J. Parravicini, C. Conti, A. J. Agranat, and E. DelRe, "Programming scale-free optics in disordered ferroelectrics," *Opt. Lett.* **37**, 2355–2357 (2012).
18. J. Parravicini, A. J. Agranat, C. Conti, and E. DelRe, "Equalizing disordered ferroelectrics for diffraction cancellation," *Appl. Phys. Lett.* **101**, 111104 (2012).
19. M. Segev, G. C. Valley, B. Crosignani, P. DiPorto, and A. Yariv, "Steady-state spatial screening solitons in photorefractive materials with external applied-field," *Phys. Rev. Lett.* **73**, 3211–3214 (1994).
20. E. DelRe, B. Crosignani, and P. Di Porto, "Photorefractive solitons and their underlying nonlocal physics," *Prog. Opt.* **53**, 153–200 (2009).
21. Z. Chen, M. Segev, and D. Christodoulides, "Optical spatial solitons: historical overview and recent advances," *Rep. Prog. Phys.* **75**, 086401 (2012).
22. S. Trillo and W. Torruellas (Eds.), *Spatial Solitons*, Vol. 82 of Springer Series in Optical Sciences (Springer, 2001).
23. Y. S. Kivshar and G. P. Agrawal, *Optical Solitons* (Academic, 2003).
24. G. P. Agrawal, *Nonlinear Fiber Optics*, 4th ed. (Academic, 2012).
25. E. DelRe, B. Crosignani, M. Tamburrini, M. Segev, M. Mitchell, E. Refaeli, and A. Agranat, "One-dimensional steady-state photorefractive spatial solitons in centrosymmetric paraelectric potassium lithium tantalate niobate," *Opt. Lett.* **23**, 421–423 (1998).
26. M. Morin, G. Duree, G. Salamo, and M. Segev, "Wave-guides formed by quasi-steady-state photorefractive spatial solitons," *Opt. Lett.* **20**, 2066–2068 (1995).
27. E. DelRe and E. Palange, "Optical nonlinearity and existence conditions for quasi-steady-state photorefractive solitons," *J. Opt. Soc. Am. B* **23**, 2323–2327 (2006).
28. C. Dari-Salisburgo, E. DelRe, and E. Palange, "Molding and stretched evolution of optical solitons in cumulative nonlinearities," *Phys. Rev. Lett.* **91**, 263903 (2003).
29. M. I. Carvalho, S. R. Singh, and D. N. Christodoulides, "Self-deflection of steady-state bright spatial solitons in biased photorefractive crystals," *Opt. Commun.* **120**, 311–315 (1995).
30. Z. G. Chen, M. Asaro, O. Ostroverkhova, and W. E. Moerner, "Self-trapping of light in an organic photorefractive glass," *Opt. Lett.* **28**, 2509–2511 (2003).
31. M. Asaro, M. Sheldon, Z. G. Chen, O. Ostroverkhova, and W. E. Moerner, "Soliton-induced waveguides in an organic photorefractive glass," *Opt. Lett.* **30**, 519–521 (2005).

1. Introduction and motivation

Understanding the glass transition is an enduring challenge, attracting continued interest [1–3]. A supercooled glass will manifest anomalous relaxation, a non-equilibrium condition that can persist in time beyond the duration of any reasonable experiment. The persistent non-equilibrium state has unique properties that can be used to achieve innovative functional materials. For example, glassy systems can have anomalously enhanced responses, such as huge viscosity, a strong history-dependence, and aging, i.e., a continuous evolution even with fixed external conditions. An expanding and promising field is that of using material complexity and glassy response to affect optical linear and nonlinear response [4, 5]. Ferroelectrics, such as LiNbO_3 , form one important class of photonic linear and nonlinear materials. Interestingly, dielectric spectroscopy indicates that a wide class of ferroelectric crystals, the so-called relaxors, manifest something that can best be understood as a glassy phase [6, 7]. In a glass, the non-equilibrium occurs between the liquid and crystalline phases, leading to the so-called glass-forming-liquid or glass-former behavior. In a glassy ferroelectric, the non-equilibrium is between the high-symmetry paraelectric and the low-symmetry polar phase, and the resulting system behaves like a dipolar glass. Glass-forming-liquid physics in relaxors is most evident in samples that have relevant compositional disorder, that is, where ions are randomly substituted in the lattice without altering the lattice geometry, for example replacing a Nb with a Ta atom in a single lattice cell of a KNbO_3 crystal. Microscopically, polar-nanoregions (PNRs) form around the compositionally disordered sites and give rise to a complex dipole-dipole interaction that ultimately causes the slowdown in relaxation and glassy behavior.

Non-stoichiometric composition has allowed the growth of variety of new optically transparent relaxors with a room-temperature glassy phase [8]. PNRs introduce a strong local anisotropy in optical response that can be oriented electrically, producing a strong electro-optic effect that affects light propagation [9–11]. When the samples are further doped with photosensitive impurities, such as Cu atoms in $K_{1-x}Li_xTa_{1-y}Nb_yO_3$ (KLTN) [12], these can allow the formation of light-induced electric fields and an ensuing strong photorefractive (PR) nonlinearity. Transparent relaxors have recently opened the way to new optical phenomena, such as scale-free propagation [13, 14] and reprogrammability of optical response [15–18].

Ferroelectrics with photosensitive impurities at equilibrium support optical PR spatial solitons [19–21], a specific example of the general class of nonlinear waves that propagate without distorting and changing [22–24]. Solitons form when material nonlinearity exactly balances linear wave-spreading processes, a fact that fixes their shape, size and intensity to the so-called soliton solution and to the “existence curve” in the wave parameter space.

To date, no study has been reported describing the behavior of solitons in a glassy system undergoing aging. In this paper we detect and study optical solitons in out-of-equilibrium super-cooled compositionally disordered Cu-doped photorefractive KNTN ($K_{1-x}Na_xTa_{1-y}Nb_yO_3$). Analyzing the conditions leading to solitons in the glassy system, we find that these change in time without relaxing to a stable time-independent state typical of equilibrium soliton formation. Whereas, in general, this leads to soliton break-up, we also observe that appropriately changing the wave parameters, i.e., normalized width and intensity, allows to compensate crystal relaxation and leads to a stable non-spreading optical waveform. Reconstructing, from these parameters, the equivalent soliton solution in the normalized width-intensity parameter plane indicates that the solution is exploring, in time, the parameter space beyond the constraints of the soliton existence curve, undergoing what can best be termed “soliton aging”.

2. Annealed versus quenched experiments

Our experiments are carried out in a transparent zero-cut $1.17^{(x)} \times 1.90^{(y)} \times 2.43^{(z)}$ mm sample with $K_{0.89}Na_{0.11}Ta_{0.63}Nb_{0.37}$. In Fig. 1(a), we report the low-frequency dielectric constant ϵ_r versus temperature T . The Curie-Weiss mean-field law breaks below $T_B = 305K$ (i.e., the Burns temperature which we can identify with the dynamical glass transition temperature) and pronounced hysteresis in the linear response is detected in proximity of $T_{max} = 285K$ where ϵ_r has its peak for the cooling trajectory. The Curie temperature is $T_C = 275K$ (fitting data for $T > T_B$ with the Curie-Weiss law $\epsilon_r = C/(T - T_C)$), and we carry out our experiments in the glass-forming-liquid region ($T_{max} < T < T_B$) at the equilibration temperature $T_e = 301K$.

The KNTN is also Cu-doped and manifest strong PR response for visible wavelengths. It is biased on the x facets with $L_x = 1.17$ mm, and its temperature T is controlled through a Peltier-junction. The crystal is initially slowly cooled to the operating temperature T_e with a cooling rate of $\alpha_a = 2.5 \cdot 10^{-3} K/s$ (annealed dipolar glass) from the initial $T_i = 310K$. It is inserted in a standard setup for the observation of one-dimensional (1D) PR screening solitons. Specifically, a Gaussian beam from a doubled-Nd-YAG laser (wavelength $\lambda = 532$ nm, power before the crystal in the soliton beam $50 \mu W$) is focused down onto the input facet of the sample and diffracts along the z axis, as shown in Fig. 1(b), from the initial minimum beam waist of $8 \mu m$ to $27 \mu m$, along the $L_z = 2.43$ mm propagation in the sample (expected Gaussian linear diffraction is $33 \mu m$ for $n_0 = 2.35$). In Figs. 1(b)–1(e) we report one example of observed beam phenomenology. As the voltage is applied, for $V = 550V$ the x -polarized (i.e., parallel to $E_0 = V/L_x$) beam converges to a soliton after 45 min when a background illumination (a co-propagating plane-wave polarized in the y -direction, orthogonal to external bias field) such that the intensity ratio $u_0^2 = I(0)/I_b = (5.2)^2$, where $I(x)$ is the beam intensity distribution and I_b the background intensity (Fig. 1(b)). The steady-state (SS) soliton appears in all identical to

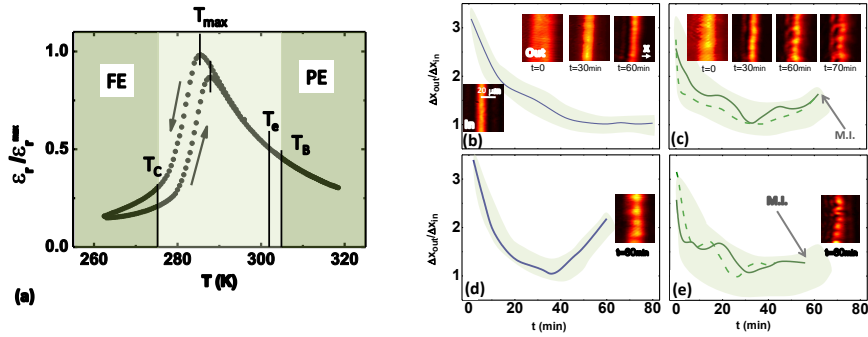


Fig. 1. Conventional PR solitons fail to form. (a) Low frequency normalized dielectric constant ϵ_r versus T manifesting thermal hysteresis for the KNTN sample. Dark-green regions indicate the paraelectric (PE) and ferroelectric (FE) ergodic (i.e., where no glassy phenomena emerge) phases, the light-green region indicates the crossing region where glassy physics emerges. (b) Steady-state screening solitons in annealed KNTN and insets reporting transverse intensity distributions of the beam at input ($z = 0$) and at the output ($z = L_z$) of the sample at different times. (c) Beam evolution in the same conditions of (b) in quenched KNTN, leading to modulation instability (M.I.) and a large variability in the trajectories (shaded region indicates the values observed in 10 successive experiments). (d) Quasi-steady-state solitons in the annealed case compared to the phenomena observed in the (e) quenched case. The slight systematic asymmetry along x in the annealed and quenched cases is caused by nonlocal terms in the response [29].

solitons generally observed in conventional ergodic ferroelectrics [25]. If the background illumination is absent (i.e., $u_0^2 \gg 1$), the beam leads to a quasi-steady-state (QSS) soliton, as shown in Fig. 1(d) [26, 27]. In turn, the glassy nature is activated through super-cooling to T_e from T_i . Specifically, in Fig. 1(c) we show the exact same experiment reported in Fig. 1(b) in conditions of cooling rate $\alpha_q = 0.07\text{K/s}$ (quenched dipolar glass), and in Fig. 1(e) we report the result for the $u_0^2 \gg 1$ case (to be compared to the Fig. 1(d) case). Evidently, the picture is fundamentally altered. In the two conditions in which the annealed case manifests SS and QSS solitons, the quenched beams appear to behave in the same manner. As expected from the general picture of an enhancement of nonlinearity due to aging, both situations lead to a runaway process that culminates and ends with beam break-up typical of modulation instability, a phenomenon normally observed either for extremely long propagation or elevated nonlinearity. Congruently, beam breakup appears on time scales that are longer than the SS soliton formation time and QSS life cycle, so the mechanism at work is intrinsically different to the conventional transient involved in QSS [28].

The impossibility of forming conventional PR solitons in the quenched dipolar glass is a flag to the fact that the nonlinear response of the material is in fact aging and changing the balance between the linear diffraction and nonlinear self-focusing, hampering the formation of a stable soliton. We repeated the experiment modifying the value of static applied voltage V but the picture is not altered in any significant way: no stable SS soliton is observed.

3. Soliton aging

Assuming therefore an aging nonlinear response for the supercooled crystal equilibrated at a fixed T_e , no truly stable soliton can form. However, as the material response changes, we can ideally change adiabatically the soliton waveform to once again satisfy the perfect balance

between diffraction and self-focusing. This would form our definition of an aging soliton. In the PR nonlinearity, this soliton aging is even more effective since the spatial scale involved in the soliton formation process is not directly the actual size of the input launched laser beam Δx , but the rescaled size $\Delta\xi = \Delta x/d$, where d depends on the applied electric field and low frequency dielectric constant ϵ_r [25]. This means that solitons have self-similar properties that allow the compensation of the aging nonlinearity without actually altering the optical waveform. In Fig. 2(a) we report the observed output intensity Δx_{out} compared to the input stabilized in time by applying the $V(t)$ and consequent bias $E_0(t)$ of Fig. 2(b). Assuming that the soliton existence parameters remain, during the process, fixed, we can deduce the equivalent hump in the ϵ_r caused by the supercooling, as shown in the lower blue curve of Fig. 2(b). The soliton solution is preserved through the transient response of the aging KNTN.

4. Discussion

We consider a material whose nonlinearity ages because of built-in disorder. Paraxial propagation is described by the generalized nonlinear Schrödinger equation [22]. The slowly varying envelope of the optical beam $A(x, z)$, localized in the x direction and diffracting along the z direction, obeys the nonlinear wave equation

$$\partial_z A(x, z) - (i/2k)\partial_{xx}A(x, z) = (ik/n_0)\Delta n(I, t)A(x, z) \quad (1)$$

where $k = (2\pi)n_0/\lambda$ is the wavenumber associated to the optical wavelength λ and unperturbed index of refraction n_0 . In general, $\Delta n(I, t)$ is the nonlinear change in index of refraction, i.e., $n = n_0 + \Delta n(I, t)$, dependent on the optical intensity $I = |A(x, z)|^2$ as well as on time, a consequence of aging. For a given t , non-spreading solutions of the general form $A(x, z, t) = A_0(t)u(x, t)\exp(i\Gamma(t)z)$ emerge only for specific waveforms and values of beam width and intensity. Since Δn evolves in time, so the conditions leading to solitons change in time, and no single input waveform and intensity will allow the formation of a stable self-trapped solution, as detected in Fig. 1. In order for a stable soliton to form, for which, for example, $u(x, t)$ does not depend on t , as demonstrated in Figs. 2(a) and 2(b), the properties of the optical wave must change in unison with the nonlinearity. For example, in the case of a Kerr nonlinearity $\Delta n = n_2(t)I$, for a given fixed beam width, or intensity Δx , the beam amplitude must become a time-dependent process so that $n_2(t)|A_0(t)|^2$ remains constant and the given $u(x, t)$ remains a time-independent soliton solution $u(x)$. Analogously, the beam width can be modified to keep the soliton on the existence curve, keeping the peak intensity constant, or both intensity and width can be changed appropriately. Biased relaxors with no polar axis manifest a quadratic electro-optic response analogous to the quadratic electro-optic effect of standard paraelectric crystals. Screening solitons are expected to obey a Kerr-like equation with a saturated nonlinearity $\Delta n = -\Delta n_0(1 + I/I_b)^{-2}$, where $\Delta n_0 = (1/2)n_0^2 g_{eff} \epsilon_0^2 (\epsilon_r - 1)^2 E_0^2$, I_b is the background illumination, g_{eff} is the effective quadratic electro-optic coefficient, ϵ_r is the low frequency relative dielectric constant, and $E_0 = V/L_x$ is the static electric field generated by the application of a voltage V on the electrodes L_x apart [25, 30, 31]. The aging phenomenon is associated to the non-ergodic behavior of $\epsilon_r = \epsilon_r(t)$, that ages and is history-dependent, as is typical for relaxors. In these conditions, the soliton equation becomes [20, 25]

$$d^2u(\xi)/d\xi^2 = -[(1 + u_0^2)^{-1} - (1 + u(\xi)^2)^{-2}]u(\xi), \quad (2)$$

where $A(x, z) = u(x)e^{i\Gamma z}\sqrt{I_b}$, $\xi = x/d$, $d = 1/\sqrt{-2kb}$, $b = (k/n_0)\Delta n_0$, and $u_0^2 = u(0)^2$ is the intensity ratio of the beam. The time parameter enters into the picture through the transverse spatial scale d (i.e., through b), which involves $\epsilon_r(t)$. Hence, on consequence of aging, $\xi = \xi(t)$. The soliton existence curve is normally cast in the $\Delta\xi$ (normalized soliton FWHM) versus u_0

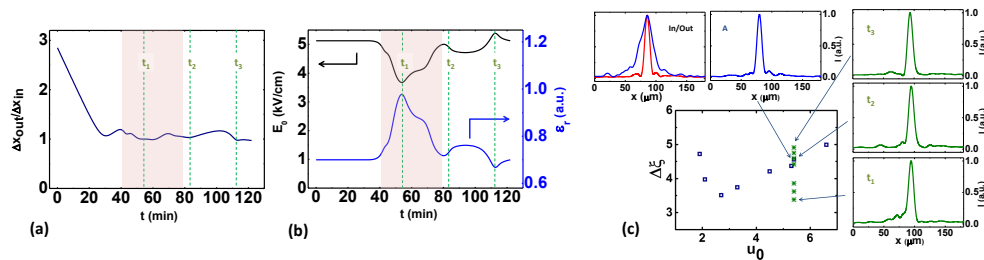


Fig. 2. Solitons that age. (a) Output FWHM indicates a stable soliton following supercooling. (b) $E_0(t)$ required to follow the soliton as the susceptibility ages and equivalent $\varepsilon_r(t)$. The shaded region indicates the transient hump in response. (c) Self-similar waveforms during the aging. (Center) Annealed existence curve (blue squares) and equivalent existence conditions for the aging KNTN in the quenched case (green asterisk points) at different instants of time, in the conditions of stabilized soliton. Insets, top-left, input (red) and output (blue) beam profiles in the linear case (at $t = 0$); top-right, output profile for a SS soliton in the annealed case in A; right, profiles of the output at t_1, t_2, t_3 .

plane (see Fig. 2(c)). As the glass-former ages, $\varepsilon_r(t)$ greatly changes, changing correspondingly $\Delta\xi$, so that for a given fixed input beam width Δx , its effective transverse size changes, and the nonlinear wave will wander in the parameter plane, in general only temporarily intersecting with the stable soliton curve. Maintaining a fixed u_0 , the soliton can be stabilized into a self-similar solution if its equivalent $\Delta\xi$ is kept constant, for example, changing in time the applied voltage V , so that $\varepsilon_r(t)V(t)$ is kept fixed, as performed in Figs. 2(a) and 2(b).

To test this picture, in Fig. 2(c) we report the annealed screening soliton existence curve (blue squares), where each point corresponds to the observation of a stable SS soliton in the annealed KNTN. As the compensated soliton evolves through the aging, the soliton itself wanders in the parameter plane, for example passing through the points indicated with the symbol “*”. These are plotted onto the plane considering the value of V applied at the given t and using the nominal ε_r at the equilibration T_e (as per Fig. 1(a)). The basic existence curve is violated. In turn, the beam profiles are self-similar, indicating that all these points actually refer to one single point in the soliton parameter plane, as the beam profiles of three selected snap-shots after the initial transient (45 min) indicate ($t_1 = 55$ min, $t_2 = 85$ min, $t_3 = 115$ min). Hence, the nonlinearity in action is not that associated with the equilibrium susceptibility, but to an aging ε_r , as discussed in Fig. 2(c), validating the general soliton aging picture.

5. Conclusions

We have experimentally analyzed what happens to solitons when the nonlinearity is relaxing. In supercooled PR transparent relaxors we have identified soliton aging, that is, the formation of a stable optical soliton waveform even as the material ages, supported by a time-dependent rescaling of soliton parameters to allow for a self-similar waveform. In terms of the general properties of soliton-supporting equations, our study sheds light on the interaction between nonlinear waves and complex states of matter.

Acknowledgements

We acknowledge experimental support from G.B. Parravicini. Research was supported by the FIRB PHOCOS-RBFR08E7VA, FILAS-SMARTCONFOCAL, and PRIN2009P3K72Z grants.

A.J.A. acknowledges the support of the Peter Brojde Center for Innovative Engineering.